Corneal biomechanical parameters of keratoconus patients from cross-meridian air-puff deformation optical coherence tomography and finite element modeling

Judith S. Birkenfeld[1*], Andrea Curatolo[2], Ashkan Eliasy[3], Eduardo Martinez-Enriquez[1], Alejandra Varea[1], Ana María Gonzalez Ramos[1], Ahmed Abass[3], Bernardo Lopes Teixeira[3], Jesus Merayo-Lloves[4], Ahmed Elsheikh[3,5,6], Susana Marcos[1,7]

[1] *Instituto de Óptica "Daza de Valdés", Consejo Superior de Investigaciones Científicas (IO, CSIC), Madrid, Spain*
[2] *Physical Optics and Biophotonics Group, Institute of Physical Chemistry, Polish Academy of Sciences, Warsaw, Poland*
[3] *Biomechanical Engineering Group, School of Engineering, University of Liverpool, Liverpool, UK*
[4] *Instituto de Oftalmobiología Aplicada, Universidad de Valladolid, Spain*
[5] *Beijing Advanced Innovation Centre for Biomedical Engineering, Beihang University, Beijing, 100083, China*
[6] *NIHR Biomedical Research Centre for Ophthalmology, Moorfields Eye Hospital NHS Foundation Trust and UCL Institute of Ophthalmology, UK*
[7] *Center for Visual Science, The Institute of Optics, Flaum Eye Institute, University of Rochester, New York, USA*
**judith.birkenfeld@io.cfmac.csic.es*

1. INTRODUCTION

Alterations in the cornea's biomechanical properties, as they occur in keratoconus (KC), lead to an abnormal corneal shape and a decreased quality of vision. It has been recognized that the measurement of the corneas´ biomechanical properties helps to diagnose corneal abnormalities earlier [1]. Currently, diagnosis, management, and treatment planning of corneal ectasia is solely based on geometrical measurements of the cornea; hence, corneal alterations are usually detected when the vision is already irreversibly affected. There is an ongoing need to improve ocular diagnostics based on biomechanical biomarkers and customized treatments. Non-contact approaches that quantify biomechanical properties *in vivo* include Optical Coherence Elastography (OCE) [2-5], Brillouin microscopy [6, 7], and air-puff deformation Scheimpflug imaging [8, 9]. Recently, Optical Coherence Tomography (OCT) devices have been coupled to air-puff excitation sources to capture the deformation event at the corneal apex or on the horizontal meridian [10-12]. Taking advantage of the OCT´s flexibility of programmable optical beam scan patterns that permit a compromise between temporal and spatial sampling of the corneal deformation profiles, we recently introduced a multi-meridian air-puff deformation ssOCT system (IMTopScanner) that is capable of acquiring dynamic corneal deformation on multiple meridians [13]. The scanning of corneal deformation under air-puff excitation beyond the horizontal meridian, which is the standard in clinical use, has the advantage in that it does not limit possible detections of corneal deformation asymmetries due to softer corneal regions below the corneal apex as they typically occur in KC patients. Additionally, it provides input data for Finite Element (FE) modeling. In this paper, we present the first results on patients with mild and moderate KC using the IMTopScanner device. We quantify deformation asymmetries on two meridians and compare them to healthy subjects. The results from the IMTopScanner, together with the subjects' intraocular pressure (IOP), topography, and biometry data were used as input data for Finite Element (FE) modeling inverse analyses via a custom-built algorithm to estimate a set of patient-specific corneal material properties.

2. METHODS AND RESULTS

Corneal air-puff deformation images from five eyes of three KC patients, and two eyes of two healthy subjects were collected using the recently developed ImTOPScanner device, a custom developed multi-meridian air-puff ssOCT system, which is described in detail elsewhere [13]. The novelty of the system is the ability to capture corneal deformation along two meridians during an air-puff excitation measurement, which allows acquisition and quantification of deformation imaging on both the horizontal and the vertical corneal axes (Fig. 1 a). All subjects were additionally measured with the Pentacam (Oculus, Wetzlar, Germany), and the IOP was measured. Custom image processing tools were used on all OCT deformation images to quantify the deformation event. The deformation data was used to extract the following deformation parameters: deflection area (DeflArea) between undeformed and deformed cornea for the horizontal and vertical scanning meridian, and the Asymmetry in DeflArea (ADA), defined as the difference between the nasal/temporal and superior/inferior DeflArea. It was further used as input data for a FE modeling inverse analysis. Therefore, patient-specific FE models were generated, based on corneal geometry, IOP and age-related scleral material properties. For KC eyes, an algorithm detected the area of pathology and allocated a separate material for the affected region [14, 15]. Through an inverse analysis procedure and simulation of air-puff pressure, corneal material stiffness for second-order Ogden material model was estimated for each patient.

KC eyes were classified into mild (three eyes) and moderate (two eyes) KC, using the Pentacam Topographic Keratoconus Classification. Two ADA parameters were further investigated: $|ADA_{max\_abs}|$, defined as the maximum absolute value of ADA during the measurement, and $|ADA_{relDif\_HV}|$, defined as the relative difference between horizontal (H) and vertical (V) ADA at maximum deformation. For the two healthy eyes, |ADAmax_abs| remained $\leq 0.20 \pm 0.02 mm^2$, for both horizontal and vertical meridian. The $|ADA_{relDif\_HV}|$ was $0.01 \pm 0.11 mm^2$ and $0.07 \pm 0.23 mm^2$. In comparison, for all KC eyes the $|ADA_{relDif\_HV}|$ was $\geq 0.14 mm^2$, i.e. up to 14 times higher than in healthy subjects. The $|ADA_{max\_abs}|$ was $>0.20 \pm 0.02 mm^2$ in all cases. Fig. 1b shows an example of the ADA for a mild and a moderate KC eye.

The patient-specific FE models estimated the tangent modulus for the eyes' materials for up to 5% strain (Fig. 1c). For KC eyes, where an area of pathology could be detected (in four out of five KC eyes), the tangent modulus was calculated inside and outside this area. At 2% strain, the tangent modulus for the cornea was estimated to be 1.34 and 1.12 MPa for healthy eyes; 1.56, 1.83, and 1.56 MPa for mild KC eyes; and 1.63, and 1.34 for moderate KC eyes. At the same strain, the tangent modulus of the area of pathology was estimated to be 1.08 and 1.35 MPa for the mild KC eyes, and 1.28 and 0.76 for moderate KC eyes. Overall, the area of pathology in KC eyes showed around 30% stiffness reduction compared to healthy areas at 2% strain.

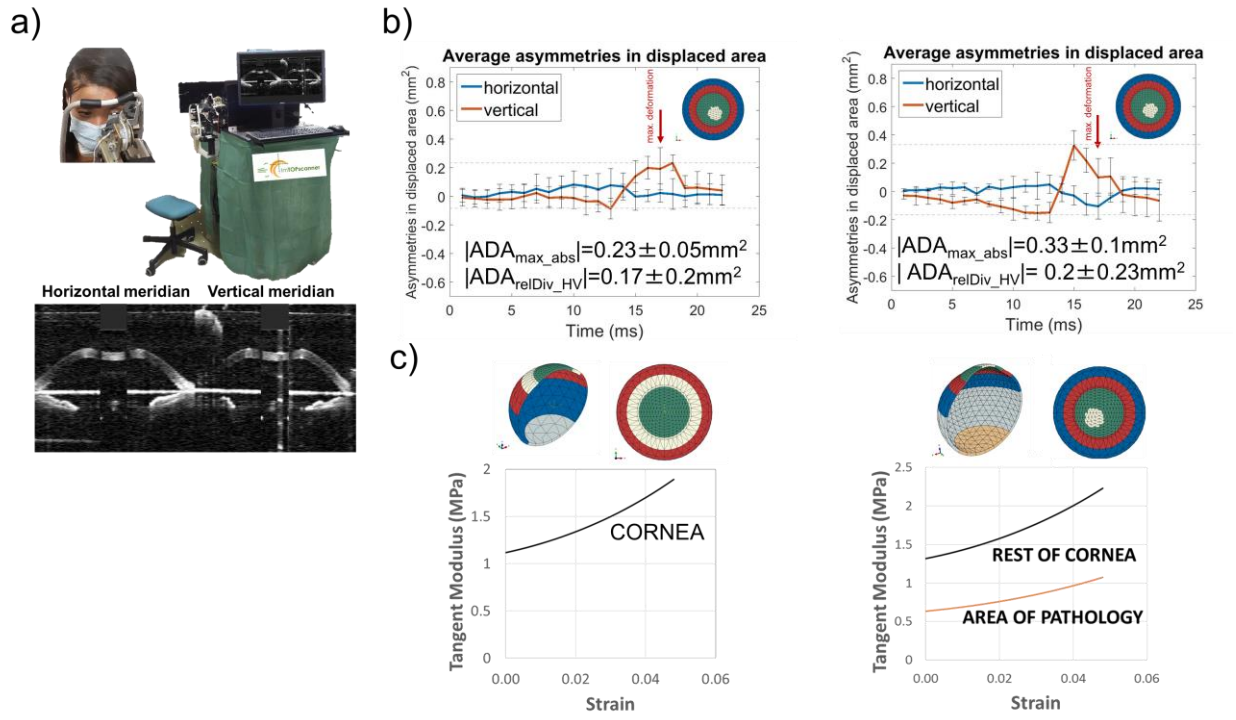

Figure 1. a) Set-up of the IMTopScanner device for patient use. Below an example-OCT image, showing the horizontal (left) and vertical (right) meridian during corneal air-puff deformation b) The average ADA for a KC patient with mild (left) and moderate (right) KC. The values for $|ADA_{relDif\_HV}|$ and $|ADA_{max\_abs}|$ are given for each eye. The time of maximum deformation is indicated with a red arrow c) Results of the FE modeling inverse analysis for a healthy (left) and moderate KC (right) subject. In the case of the KC eye, an area of pathology was detected, and a separate material for the affected region was allocated.

REFERENCES

1. Edmund, Carsten, *Acta ophthalmologica* 66.2 (1988): 134-140.
2. Larin, Kirill V., and David D. Sampson, *Biomedical optics express* 8.2 (2017): 1172-1202.
3. Jin, Zi, et al., *Journal of biophotonics* 13.8 (2020): e202000104.
4. Ramier, Antoine, et al., *Optics express* 27.12 (2019): 16635-16649.
5. Ramier, Antoine, et al., *Scientific reports* 10.1 (2020): 1-10.
6. Scarcelli, Giuliano et al., *Investigative ophthalmology & visual science* 53.1 (2012): 185-190.
7. Shao, Peng, et al., *Scientific reports* 9.1 (2019): 1-12.
8. Eliasy, Ashkan, et al., *Frontiers in bioengineering and biotechnology* 7 (2019): 105.
9. Roberts, Cynthia J., et al., *Journal of refractive surgery* 33.4 (2017): 266-273.
10. Alonso-Caneiro, David, et al., *Optics express* 19.15 (2011): 14188-14199.
11. Dorronsoro, Carlos, et al., *Biomedical optics express* 3.3 (2012): 473-487.
12. Jiménez-Villar, Alfonso, et al., *Biomedical optics express* 10.7 (2019): 3663-3680.
13. Curatolo, Andrea, et al., *Biomedical optics express* 11.11 (2020): 6337-6355.
14. Eliasy, Ashkan, et al., *Journal of the Royal Society Interface* 17.169 (2020): 20200271.
15. Lopes, Bernardo, et al., *Journal of Refractive Surgery* 37.6 (2021): 414-421.